Sensors and Materials, Vol. 35, No. # (2023) 1–##
MYU Tokyo

S & M ####

Observation of Surface Potential of Micropatterned Self-assembled Electrets for MEMS Vibrational Energy Harvesters

Daisuke Yamane,[1,2*] Kosuke Kawashima,[1] Reiki Sugimoto,[1] Ruichen Li,[2] Hideyuki Kayaguchi,[3] Keisuke Kurihara,[3] Hisao Ishii,[3,4] and Yuya Tanaka[5]

[1]Graduate School of Science and Engineering, Ritsumeikan University, 1-1-1 Noji-Higashi, Kusatsu, Shiga 525-8577, Japan
[2]Department of Mechanical Engineering, College of Science and Engineering, Ritsumeikan University, 1-1-1 Noji-Higashi, Kusatsu, Shiga 525-8577, Japan
[3]Graduate School of Science and Engineering, Chiba University, 1-33 Yayoi-cho, Inage-ku, Chiba 263-8522, Japan
[4]Center for Frontier Science, Chiba University, 1-33 Yayoi-cho, Inage-ku, Chiba 263-8522, Japan
[5]Graduate School of Science and Technology, Gunma University, 1-5-1 Tenjin-cho, Kiryu, Gunma 376-8515, Japan

(Received March 23, 2023; accepted May 11, 2023)

Keywords: micropattern, self-assembled electret, MEMS, vibration, energy harvester

In this paper, we present the observation results of the surface potential of micropatterned thick (> 1 μm) self-assembled electrets (SAEs) for MEMS vibrational energy harvesters (VEHs). To evaluate the surface potential of micropatterned SAEs, we propose and develop test devices with removable through-hole substrates corresponding to the moving electrodes of SAE-MEMS VEHs. In this study, SAEs are deposited simultaneously on two test devices with different through-hole spacings and on a reference flat substrate using the same vacuum evaporation process. The surface potential of SAEs is proportional to the film thickness, and when the film thickness of the SAE deposited on the flat substrate is 4.48 μm, the surface potential exceeds 200 V. At this time, in a test device where the average thickness of micropatterned SAEs is 3.08 μm, the measured surface potential is 68 V. In addition, it is experimentally observed that when micropatterned SAEs are formed using the through-hole structures, the microfabrication process causes the SAE pattern to spread wider than the through-hole dimensions, and the surface profiles are not flat. These findings provide useful insights for the design of SAE-MEMS VEHs using micropatterned SAEs with through-hole structures.

1. Introduction

Energy harvesting is a technology that transforms various types of microenvironmental energy that exists around us into electrical energy.(1) Among these types, environmental vibration exists both indoors and outdoors, day and night. Consequently, vibrational energy harvesters (VEHs) can be important devices for powering microsystems such as low-power wireless sensor nodes.(2–4) Among several technologies for transforming vibration energy into

*Corresponding author: e-mail: dyamane@fc.ritsumei.ac.jp
https://doi.org/10.18494/SAM4400

ISSN 0914-4935
https://myukk.org/

electricity, electrostatic VEHs using electrets have a comparatively wide operating frequency range and a moderate power density; moreover, they can be miniaturized with MEMS technology.[5,6] Conventional electrets require process temperatures of 100 °C or higher during film deposition[7] or charging.[5,6] In addition, conventional electret charging processes require the application of several hundred to several thousand volts and sometimes X-ray irradiation.[8]

Recently, self-assembled electrets (SAEs), which are electrets that do not require any charging process, have been developed.[9] The surface potential of the SAE film appears owing to the spontaneous orientation of dipole of polar organic molecules, and thus the potential linearly increases with the film thickness.[10,11] SAEs can be deposited at room temperature by vacuum evaporation, which allows for the possibility of integrating electrostatic VEHs with a variety of elements. For the miniaturization and electric circuit monolithic integration of VEHs, we have recently succeeded in forming SAEs inside MEMS vibration devices and realized SAE-MEMS VEHs.[12] The next challenge is to directly measure and evaluate the surface potential of micropatterned SAEs inside MEMS structures to enable the precise design of SAE-MEMS VEHs. In our previous report,[13] we evaluated the surface potential and line profiles of thin (< 100 nm) micropatterned SAEs; since the surface potential of SAEs is proportional to the film thickness,[9-11] the surface potential at that time was about 2 V, and we have not confirmed the surface potential to be more than several tens of volts, which is common for electret-type MEMS VEHs. Furthermore, the three-dimensional profile of the micropatterned SAE could not be evaluated. In this paper, we report observation results of surface potentials and three-dimensional surface profiles for thick-film (> 1 μm) micropatterned SAEs that are capable of generating surface potentials of several tens of volts or more.

2. Methods

Figure 1 shows a schematic illustration of the SAE-MEMS VEH developed by our group.[12] In this device, micropatterned SAEs are formed on the substrate by the vacuum evaporation of SAEs from above the movable electrode with through holes. The surface potential of these micropatterned SAEs generates induced charges on the movable electrode, and the amount of induced charges changes when the device vibrates, enabling vibrational power generation. When

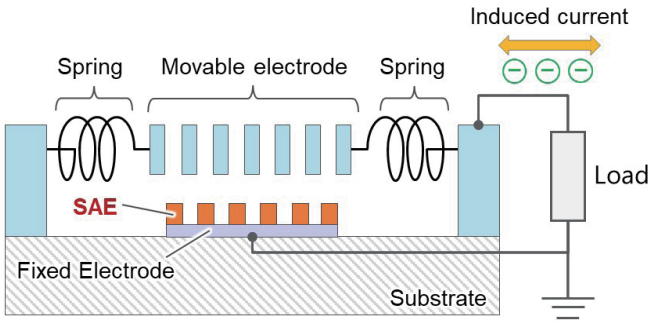

Fig. 1. (Color online) MEMS vibrational energy harvester with self-assembled electrets.

SAEs are formed inside SAE-MEMS VEH devices, the surface potential of those SAEs cannot be measured directly because the moving electrodes would interfere with the measurement. The output power is proportional to the square of the surface potential of electrets,[14] and thus the evaluation of the surface potential of micropatterned SAEs is essential for the accurate design of SAE-MEMS VEHs. To solve this problem, we propose a test device as shown in Fig. 2. The first step is to prepare Si through-hole structures for the micropatterning of SAEs simultaneously with vacuum evaporation. A 500-μm-thick Si substrate is thinned down to 100 μm (t = 100 μm) and then through holes are formed using deep reactive ion etching technology. For the previously reported SAE-MEMS VEH device,[12] the thickness of the movable electrode with the through-hole structure was 30 μm. In the future, we expect that the through-hole structure will be made thicker in order to achieve a higher output power of the VEH. Therefore, at this time, the thickness of the through-hole structure was set to 100 μm, also considering the ease of handling during the microfabrication process. As with the through-hole structures of the previous SAE-MEMS VEH device,[12] the through-hole structure was designed to have an aspect ratio between 1 and 2, with one type of w_h (80 μm) and two types of w_s (40 and 80 μm) as shown in Fig. 2(1). Next, the developed through-hole structure was attached to the substrate via spacers of thickness h [Fig. 2(1)]. The upper limit of SAE film thickness in our vacuum deposition equipment was estimated to be about 5 μm, and therefore h was set to be 10 times higher than the maximum SAE film thickness, which was 50 μm. In this study, 50-μm-thick polyimide Kapton tapes were

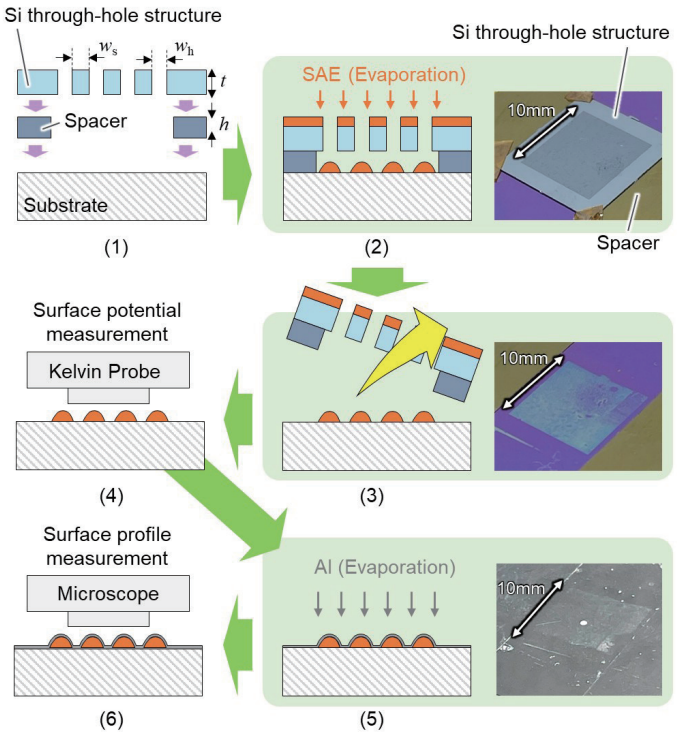

Fig. 2. (Color online) Development of test device to measure surface potential and surface profile of micropatterned SAEs formed using through-hole structures.

used as spacers. The same Kapton tapes were also used to fix the through-hole structure on the substrate. An SAE was then vacuum-deposited from above the through-hole structure [Fig. 2(2)]. This SAE deposition process has been reported elsewhere.[12] After SAE deposition, the through-hole structure was removed from the substrate [Fig. 2(3)]. This allows the surface potential of micropatterned SAEs to be measured directly with a Kelvin probe [Fig. 2(4)]. In addition, laser microscopy observation was performed to precisely evaluate the three-dimensional shape of the micropatterned SAEs. SAEs do not reflect the laser of the microscope; thus, a thin Al film was deposited on the surface of the SAE by vacuum evaporation [Fig. 2(5)]. This allows the quantitative evaluation of the surface profile of micropatterned SAEs using the laser microscope [Fig. 2(6)].

Photographs (2), (3), and (5) in Fig. 2 show an example of the developed test devices; a thermally oxidized Si substrate was used as the substrate to visually confirm the SAE. By using a shadow mask during SAE deposition, the SAE deposition area was limited to only the area of the through-hole structure.

3. Results and Discussion

The micropatterned SAEs developed for surface potential and surface profile evaluation [corresponding to Fig. 2(3)] are shown in Fig. 3. In this experiment, Alq_3 (unsublimed, purity > 98.0%, Tokyo Chemical Industry Co., Ltd.) was used for the SAEs and deposited via thermal evaporation with a base pressure of 4×10^{-4} Pa at room temperature. Glass substrates with 150-nm-thick indium tin oxide (ITO) films were used as the sample substrates to correctly measure the surface potential of the SAEs. Samples A [Fig. 3(a)] and B [Fig. 3(b)] have SAE films deposited simultaneously using the same vacuum evaporation process. For the design values of w_h and w_s [Fig. 2(1)], they were 80 and 80 μm for sample A and 80 and 40 μm for sample B, respectively. The actual dimension of one side of the through-hole developed was 85 μm, and the actual dimension of one side of the SAE films deposited in samples A and B was

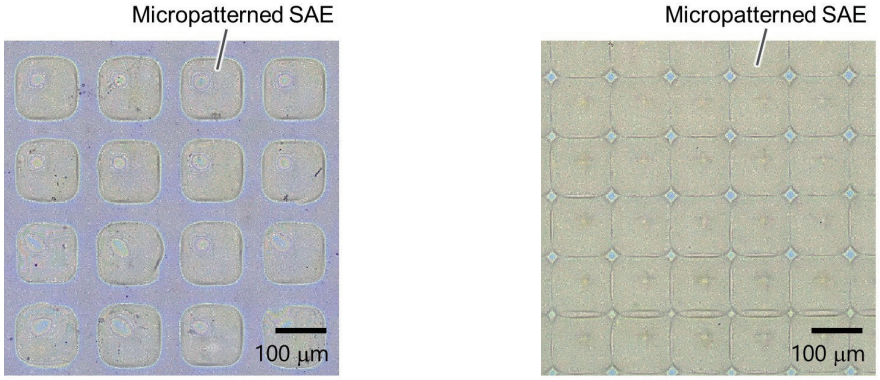

(a) (b)

Fig. 3. (Color online) Photographs of developed micropatterned SAEs before Al deposition. (a) Sample A and (b) sample B.

around 122 μm. We can therefore observe that the size of the micropatterned SAEs is larger than the through-hole dimensions. As a result, for example, in sample B [Fig. 3(b)], where the spacing between through holes is narrow, some of the adjacent SAE films overlap each other. Therefore, the results of the SAE film thickness evaluation are also discussed later in this section.

The surface potentials of the micropatterned SAEs were measured using a Kelvin probe (UHVKP020, KP Technology) with a tip diameter of 6 mm. The diameter of the Kelvin probe tip is larger than the micropatterned individual SAE films, and therefore, in this case, the average surface potential within the probe area was measured. To suppress the effects of atmospheric light and humidity, the samples after deposition were moved into a glove box (KK-1841, KIYON) connected to vacuum deposition equipment and evaluated under dark room conditions. During surface potential measurement, the ITO films under the SAEs were electrically grounded. The surface potentials of samples A and B were 16.6 and 68.2 V, respectively. At that time, the surface potential of an SAE film on a flat substrate deposited at the same time was 213.1 V. Regarding the flat SAE film, the thickness was measured to be 4.48 μm using a profilometer (ET4000A, Kosaka Laboratory). Note that the surface potential of the SAE is proportional to the SAE film thickness.[9,15] Since the actual surface potentials of samples A and B are different, their film thicknesses are considered to be different from each other, although they were fabricated by the same vacuum evaporation process. Moreover, the flat SAE film thickness is considered to be different from the actual thickness of the micropatterned SAE films because of the shadow mask with the through-hole structure.

Laser microscopy observations were performed to evaluate the surface profile and actual film thickness of the developed micropatterned SAEs. Thin Al films were deposited on the surfaces of the SAE films because the SAEs transmit the laser light of the laser microscope. The SEM images of samples A and B obtained before and after Al deposition are shown in Fig. 4. The Al films were deposited by vacuum evaporation with a thickness of 43 nm. The SAE itself is almost a dielectric material, resulting in slightly blurred contours in the image during SEM observation before Al deposition [Figs. 4(a) and 4(b)]. On the other hand, clear SEM images were obtained for the Al-coated SAE films [Figs. 4(c) and 4(d)]. The surface profiles of Al-deposited samples A and B were observed using a laser microscope (VK-X3050, KEYENCE), and the results are shown in Fig. 5. This observation revealed that the surface profiles of the micropatterned SAEs deposited through the through-hole structure are not planar. In sample A [Fig. 5(a)], a dimple can be seen within each SAE film. This might be due to the substrate rotation during the evaporation or the sample not being level during SAE deposition. The position of the evaporation source and the samples changed over time because the evaporation was performed while rotating the substrate on which the samples were fixed. When the distance between the samples and the evaporation source increases, the evaporation material tends to spread under the through-hole structure. The vertical distance from the evaporation source to the samples is 222 mm, and the horizontal distances between the samples and the evaporation source are 35.1 mm at the closest point and 84.8 mm at the furthest distance. Therefore, the SAE enters at an angle of incidence between 8.98 and 20.9° to the samples. Thus, when the spacer height of the sample is 50 μm, as in this case, the SAE patterns extend about 19.1 μm below the through-hole structure when the sample and the evaporation source are farthest apart. As

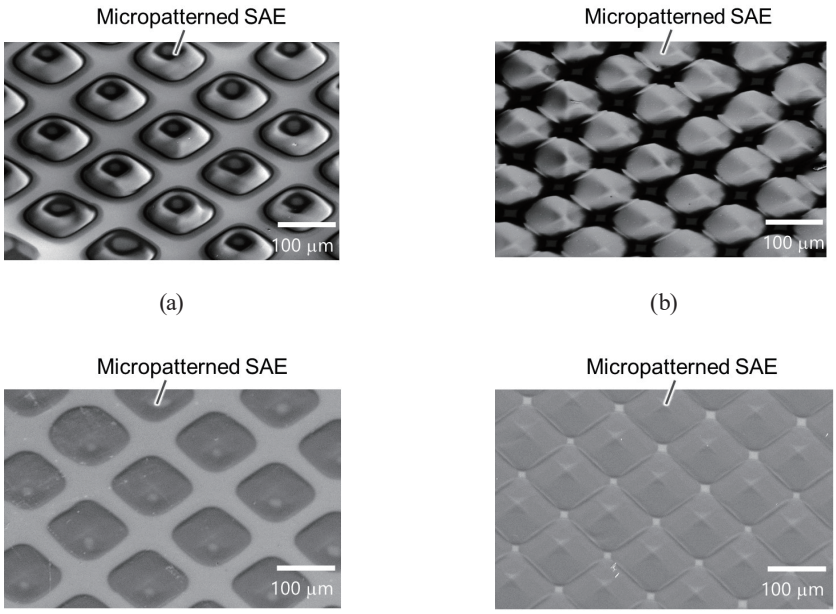

Fig. 4. (Color online) SEM images of developed micropatterned SAEs. (a) Sample A before Al deposition, (b) sample B before Al deposition, (c) sample A after Al deposition, and (d) sample B after Al deposition.

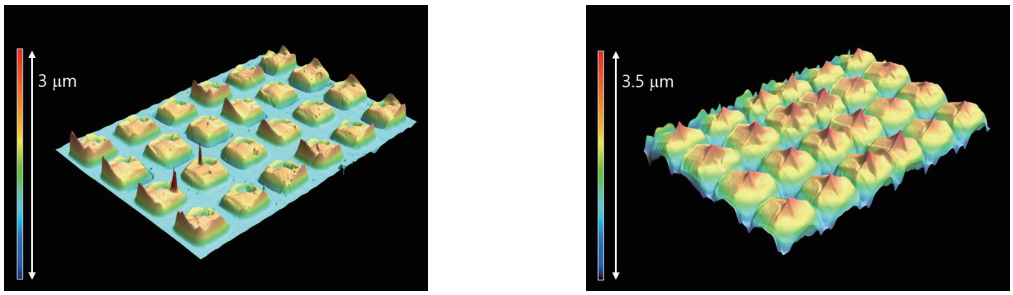

Fig. 5. (Color online) 3-D profile images of developed micropatterned SAEs after Al deposition. (a) Sample A and (b) sample B.

mentioned at the beginning of this chapter, the actual measured value of one side of the through-hole was 85 μm, and considering the spread of the SAE patterns, one SAE side can be estimated to be approximately 85 + 19.1 × 2 = 123 μm. Since this estimated value is almost the same as the measurement result (122 μm), this discussion could be valid. Similarly, in sample B [Fig. 5(b)], the SAE film thickness was nonuniform within each pattern. Nevertheless, the contour shape of each SAE film corresponding to the through-hole pattern can still be clearly seen. The improvement of the planarity of micropatterned SAE films can be possible by precisely leveling the device at SAE deposition. For each sample, the SAE average film thickness in the range observed by laser microscopy (Fig. 5) was evaluated using the microscope's image processing

function. As a result, the average film thicknesses of samples A and B were 1.55 and 2.96 μm, respectively. In the evaporation chamber, samples A and B were placed in a position where the same SAE thickness would be deposited under ideal conditions. Actual results showed that even with the same through-hole dimensions, different through-hole spacings resulted in different average film thicknesses. Future evaluations of the thickness and shape of SAE films formed by shadow masks with through holes of various sizes, shapes, and densities are needed to clarify the cause of the differences in the shape and average thickness of each pattern in samples A and B.

The measured SAE film thickness and surface potential for samples A and B, as well as for the reference SAE flat film, are summarized in Fig. 6. The flat film with the SAE deposited on the substrate without through-hole structures was formed by the same process as samples A and B. The surface potential of the SAE flat film is proportional to the film thickness, with a proportionality factor of 47 V/μm. This proportionality factor is comparable to the previously reported value for Alq_3 (50 V/μm),[11] indicating the validity of the SAE deposition process.

For such patterns of electrets, the effects of the distortion of the lines of electric force need to be considered. The electrostatic field simulation of this case was investigated using a finite-element-method simulator, COMSOL Multiphysics 6.1. Two-dimensional simulation results for the SAE flat film and samples A and B are shown in Fig 7. The film thickness for each model was set as the measured average thickness, and the pattern width and spacing for samples A and B were set as the design dimensions. All the substrates were glass substrates with ITO deposited on them, as used in the experiments, and the ITO films on their surfaces were electrically grounded. The surface charge density and dielectric constant of the SAE (Alq_3) were previously reported values.[16] Since the distance between the SAE surface and the Kelvin probe was about 300 μm, the position 300 μm above the SAE surface is shown in each figure in Fig. 7. The simulation results showed that the surface potential in this measurement was at a position where the effect of the distortion of the lines of electric force for samples A and B could be almost negligible.

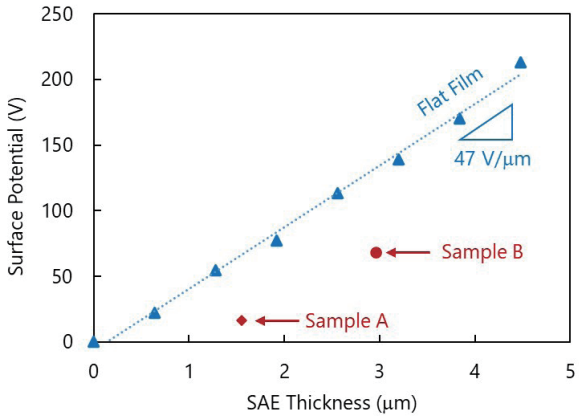

Fig. 6. (Color online) Measured results of relationship between SAE surface potential and SAE film thickness.

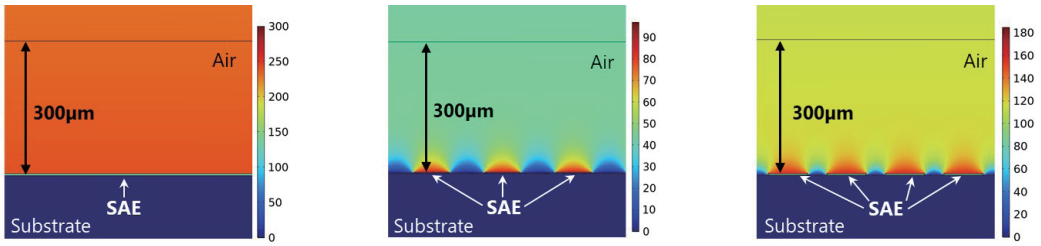

(a) (b) (c)

Fig. 7. (Color online) Electric field analysis results on SAE. The SAE thickness for each model was the average of the measured thicknesses. The pattern width and spacing for samples A and B were design dimensions. (a) Flat film, (b) sample A, and (c) sample B.

The differences in surface potential characteristics between the micropatterned SAEs and the SAE flat films may be due to the fact that the surface profiles of the micropatterned SAEs are not flat. The surface potential of the micropatterned SAE films is smaller than that of the SAE flat films, suggesting that some of the lines of electric force generated by the micropatterned SAE films might be terminated in the underlying ITO film. As mentioned earlier, increasing the SAE surface potential is useful for increasing the output power of SAE-MEMS VEHs.[10,15] The results of this study indicate that the average surface potential of the micropatterned SAE is not only determined by the average thickness but also affected by the surface profile of each pattern. Further investigation is required to clarify the relationship between the surface potential and shape of each pattern. We believe that optimizing micropatterned SAEs offers the prospect of increasing the output power of SAE-MEMS VEHs.

4. Conclusions

We proposed test devices to evaluate the surface potential of micropatterned thick SAEs for MEMS VEHs. Two types of test device and a reference flat substrate were used for the evaluation. At the SAE film thickness of 4.48 μm deposited on a flat substrate, the surface potential exceeded 200 V, and its proportionality coefficient was comparable to previously reported values, confirming the validity of the SAE deposition process used. Regarding the test devices deposited at the same time, the measured surface potential was 68 V for the micropatterned SAEs with an average thickness of 2.96 μm. Furthermore, we experimentally observed that when SAEs were micropatterned using the through-hole structures, the substrate rotation of the evaporation spread the SAE patterns wider than the through-hole dimensions, and the surface profiles were not flat. These findings can be useful for the development of SAE-MEMS VEHs that use micropatterned SAEs with through-hole structures.

Acknowledgments

This work was supported in part by the Adaptable and Seamless Technology Transfer Program through Target-driven R&D (A-STEP) from the Japan Science and Technology Agency (JST) Grant Number JPMJTR22R5, JST CREST Grant Number JPMJCR21Q2, JSPS KAKENHI 22H01929, 21K05208, and 20H02810, and a Grant-in-aid by Samco Foundation, Japan.

References

1 H. Akinaga: Jpn. J. Appl. Phys. **59** (2020) 110201. https://doi.org/10.35848/1347-4065/abbfa0
2 S. Roundy, P. K. Wright, and J. Rabaey: Meas. Sci. Technol. **26** (2003) 1131. https://doi.org/10.1016/S0140-3664(02)00248-7
3 S. P. Beeby, M. J. Tudor, and N. M. White: Meas. Sci. Technol. **17** (2006) R175. https://doi.org/10.1088/0957-0233/17/12/R01
4 P. D. Mitcheson, E. M. Yeatman, G. K. Rao, A. S. Holmes, and T. C. Green: Proc. IEEE **96** (2008) 1457. https://doi.org/10.1109/JPROC.2008.927494
5 Y. Suzuki: IEEJ Trans. Elec. Electron. Eng. **6** (2011) 101. https://doi.org/10.1002/tee.20631
6 H. Toshiyoshi, S. Ju, H. Honma, C.-H. Ji, and H. Fujita: Sci. Technol. Adv. Mater. **20** (2019) 124. https://doi.org/10.1080/14686996.2019.1569828
7 M. Honzumi, K. Hagiwara, Y. Iguchi and Y Suzuki: Appl. Phys. Lett., **98** (2011) 052901. https://doi.org/10.1063/1.3548866
8 K. Hagiwara, M. Goto, Y. Iguchi, T. Tajima, Y. Yasuno, H. Kodama, K. Kidokoro, and Y. Suzuki: Trans. IEEE Dielectr. Electr. Insul. **19** (2012) 1291. https://doi.org/10.1109/TDEI.2012.6260003
9 Y. Tanaka, N. Matsuura, and H. Ishii: Sci. Rep. **10** (2020) 6648. https://doi.org/10.1038/s41598-020-63484-9
10 Y. Noguchi, Y. Tanaka, H. Ishii, and W. Brütting: Synth. Met. **288** (2022) 117101. https://doi.org/10.1016/j.synthmet.2022.117101
11 E. Ito, Y. Washizu, N. Hayashi, H. Ishii, N. Matsuie, K. Tsuboi, Y. Ouchi, Y. Harima, K. Yamashita, and K. Seki: Appl. Phys. Lett., **98** (2002) 7306. https://doi.org/10.1063/1.1518759
12 D. Yamane, H. Kayaguchi, K. Kawashima, H. Ishii, and Y. Tanaka: Appl. Phys. Lett. **119** (2021) 254102. https://doi.org/10.1063/5.0072596
13 K. Kawashima, R. Sugimoto, R. Li, H. Kayaguchi, K. Kurihara, H. Ishii, Y. Tanaka, and D. Yamane: Proc. 21st Int. Conf. Micro and Nanotechnology for Power Generation and Energy Conversion Applications (PowerMEMS 2022) (2022) 307. https://doi.org/10.1109/PowerMEMS56853.2022.10007570
14 S. Boisseau, G. Despesse, and A. Sylvestre: Smart Mater. Struct. **19** (2010) 075015. https://doi.org/10.1088/0964-1726/19/7/075015
15 Y. Tanaka, N. Matsuura, and H. Ishii: Sens. Mater. **34** (2022) 1859. https://doi.org/10.18494/SAM3860
16 Y. Noguchi, Y. Miyazaki, Y. Tanaka, N. Sato, Y. Nakayama, T. D. Schmidt, W. Brütting, and H. Ishii: J. Appl. Phys. **111** (2012) 114508. http://dx.doi.org/10.1063/1.4724349